LBL-32481
UC-414

Lawrence Berkeley Laboratory
UNIVERSITY OF CALIFORNIA

Accelerator & Fusion
Research Division

Presented at the SPIE's International Symposia on
Laser Engineering, Los Angeles, CA, January 16–23, 1993,
and to be published in the Proceedings

Three-Dimensional Simulation Analysis of the Standing-wave Free-electron Laser Two Beam Accelerator

C. Wang and A. Sessler

January 1993

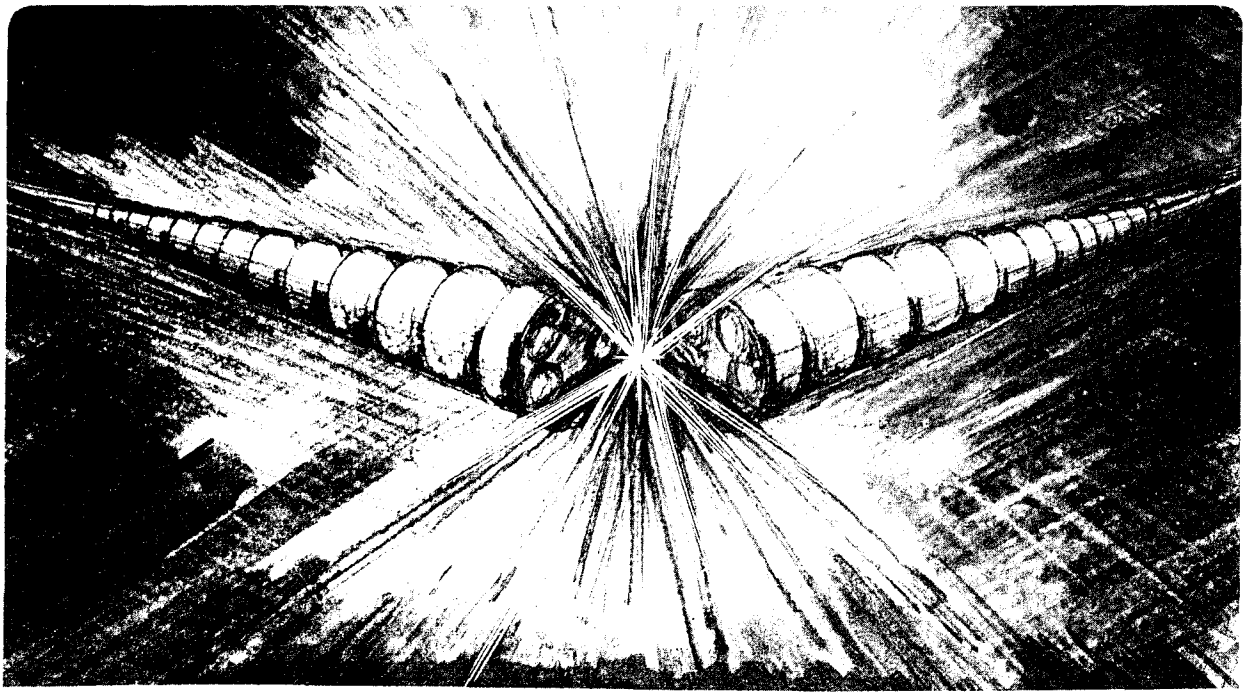

Prepared for the U.S. Department of Energy under Contract Number DE-AC03-76SF00098

LBL-32481
ESG-199
UC-414

Three-Dimensional Simulation Analysis of the Standing-wave Free-electron Laser Two Beam Accelerator*

Changbiao Wang and Andrew Sessler

Lawrence Berkeley Laboratory, University of California, Berkeley, CA 94720

January 1993

* Work supported by the Director, Office of Energy Research, Office of High Energy and Nuclear Physics, Division of High Energy Physics, of the U.S. Department of Energy under Contract No. DE-AC03-76SF00098.

Three-dimensional simulation analysis of the standing-wave free-electron laser two beam accelerator*

Changbiao Wang[a] and Andrew M. Sessler

Lawrence Berkeley Laboratory
University of California, Berkeley, California 94720

ABSTRACT

We have modified a two-dimensional relativistic klystron code, developed by Ryne and Yu, to simulate both the standing-wave free-electron laser two-beam accelerator and the relativistic klystron two-beam accelerator. In this paper, the code is used to study a standing-wave free-electron laser with three cavities. The effect of the radius of the electron beam on the RF output power; namely, a three-dimensional effect is examined.

1. INTRODUCTION

To date, investigations on the standing-wave free-electron laser two-beam accelerator (SWFEL/TBA) and the relativistic klystron two-beam accelerator (RK/TBA) have been made based on one-dimensional analysis.[1-5] The two-dimensional, time-dependent simulation code RKTW2D, developed by Ryne and Yu,[6] has been used to design a reacceleration experiment at LLNL.[7] We have modified the code to simulate both the SWFEL/TBA and the RK/TBA. We call the modified code RKFEL and it is described in section 2. This code is used to study a particular three-cavity free-electron laser described in section 3. The beam RF current as a function of longitudinal distance and the time profile of the RF output power are calculated in section 4. The effect of the radius of an electron beam on the RF output power is examined in section 5.

2. BASIC EQUATIONS FOR RKFEL

Unlike a klystron where an electron beam loses its energy by the coupling of the longitudinal velocity with the longitudinal component of the RF electric field, the SWFEL employs an electron beam with a transverse wiggle motion to interact with the transverse electric fields. The electron equations of motion for RKFEL must include both the transverse and longitudinal electric fields and they are written as[8]

$$\frac{dx}{dz} = v_x, \tag{1}$$

$$\frac{dy}{dz} = v_y, \tag{2}$$

$$\frac{d\phi}{dz} = \omega/v_z, \tag{3}$$

$$\frac{dv_x}{dz} = \frac{e}{\gamma m v_z}\left[\left(\mathbf{E} + \mathbf{V}\times\mathbf{B}\right)_x - \mathbf{v}.\mathbf{E}v_x\right], \tag{4}$$

$$\frac{dv_y}{dz} = \frac{e}{\gamma m v_z}\left[\left(\mathbf{E} + \mathbf{V}\times\mathbf{B}\right)_y - \mathbf{v}.\mathbf{E}v_y\right], \tag{5}$$

$$\frac{d\gamma}{dz} = \frac{e}{mc^2 v_z}\mathbf{v}.\mathbf{E}, \tag{6}$$

where e is the electron charge, $\phi=\omega t$ with ω the drive frequency, and v_z is determined from the usual formula for γ; namely $\gamma=\left[1-(v_x^2+v_y^2+v_z^2)/c^2\right]^{-1/2}$ with c the light speed in free space. In Eqs.(1)-(6), we take x, y, ϕ, v_x, v_y, and γ as dependent variables, and take z as the independent variable. The electromagnetic fields in the above equations are given by

$$\mathbf{E} = \mathrm{Re}\left[i\omega b_n \mathbf{A}_n(\mathbf{x})\, e^{-i\omega t}\right], \qquad \mathbf{B} = \mathrm{Re}\left[b_n \nabla\times\mathbf{A}_n(\mathbf{x})\, e^{-i\omega t}\right], \tag{7}$$

---

* The work was supported by the Director, Office of Energy Research, Office of High Energy and Nuclear Physics, Division of High Energy Physics, of the U. S. Department of Energy under Contract No. DE-AC03-76SF00098.

[a] Permanent address: High Energy Electronics Research Institute, University of Electronic Science and Technology of China, Chengdu, Sichuan 610054, China.

where $\mathbf{A}_n(\mathbf{x})$ is the eigen-mode vector potential for the n^{th} cell of a traveling wave structure or a standing wave structure and b_n is the beam-wave coupling function. For this version of RKFEL, the eigen-mode fields of the SWFEL are produced by a regular cylindrical cavity operating in the TE_{11q} mode, but we are developing the capability of employing more general fields, as is the case in RKTW2D. The beam-wave coupling function satisfies

$$\ddot{b}_n + \left(\frac{\omega_n}{Q_n} - 2i\omega\right)\dot{b}_n + \left(\omega_n^2 - \omega^2 - \frac{i\omega\omega_n}{Q_n}\right)b_n - \left(K_n^{n-1}b_{n-1} - K_n^{n+1}b_{n+1}\right) = \mu_0 c^2 \int_{\text{nth cell}} \mathbf{J}_1(\mathbf{x}).\mathbf{A}_n(\mathbf{x})\, d^3\mathbf{x}_n, \tag{8}$$

where $Q_n = Q_{nw}Q_{ne}/(Q_{nw}+Q_{ne})$ is the loaded quality factor with Q_{nw} and Q_{ne} the wall-dissipated and external quality factors respectively, ω_n is the n^{th} cell's resonance frequency, K_n^{n-1} is the cell-to-cell coupling coefficient, and μ_0 is the vacuum permeability. The Fourier component $\mathbf{J}_1(\mathbf{x})$ is defined by

$$\mathbf{J}_1(\mathbf{x}) = \frac{1}{\pi}\int_{-\pi}^{\pi} \mathbf{J}(\mathbf{x},t)\, e^{i\left[\frac{\omega_n}{\omega}\right]\omega t}\, d(\omega t), \tag{9}$$

where $\left[\frac{\omega_n}{\omega}\right]$ denotes the integer most near ω_n/ω.

The main difference between the basic equations of RKTW2D and RKFEL is that RKFEL takes into account the effects of the transverse fields on the motion of electrons and the beam-wave coupling function.

3. DESCRIPTION OF A PARTICULAR SWFEL

So as to be specific, we have taken, as shown in Fig. 1, the SWFEL have three identical cavities with a radius of 5.71 cm and a length of 80 cm, and a resonance frequency of 17.12 GHz, operating in the $TE_{1,1,91}$ mode. This situation is closely similar to that used, in experiments, with a relativistic klystron where either longitudinal bunching or transverse chopping was employed. To shorten the start-up time, we input a power of 1 kW in the first cavity. The drift tubes with a radius of 2 cm provide passage for a 1-kA, 5-MeV electron beam immersed in a combined wiggler magnetic field. In the first 140-cm drift tube, we use seven tapered magnetic wiggler periods to make the electron beam move in helical orbits. In the other two 20-cm drift tubes and three cavities, the wiggler amplitude is uniform.

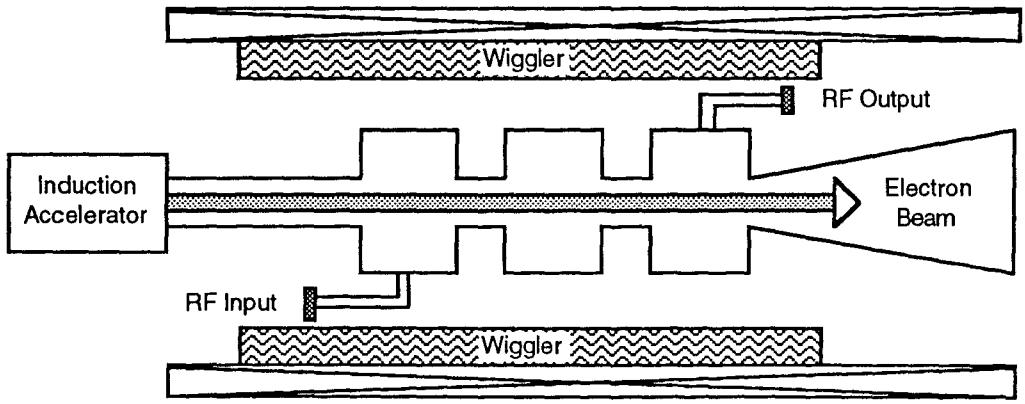

Fig. 1. Diagram of the three-cavity free-electron laser

The combined wiggler magnetic field is expressed by the following analytic formula

$$B_x = T(z)B_{w0}[I_0(k_w r)\cos(k_w z) + I_2(k_w r)\cos(k_w z - 2\theta)], \tag{10}$$

$$B_y = T(z)B_{w0}[I_0(k_w r)\sin(k_w z) - I_2(k_w r)\sin(k_w z - 2\theta)], \tag{11}$$

$$B_z = -2T(z)\, B_{w0} I_1(k_w r)\sin(k_w z - \theta) + B_0, \tag{12}$$

where B_{w0} is the wiggler amplitude on the axis, B_0 is the axial uniform magnetic field, the wiggler wave number is given by $k_w=2\pi/\lambda_w$ with λ_w the wiggler period, and the tapering factor is given by $T(z)=z/7\lambda_w$ when $z\le 7\lambda_w$ and $T(z)=1$ when $z>7\lambda_w$. We take B_{w0}=3500 Gauss and λ_w=20 cm.

Firstly, we use the cavity resonance condition to make choice of a proper cavity radius for a given operating frequency of 17.12 GHz in the TE_{11q} mode. For a cavity radius of 5.71 cm, the longitudinal mode index q is 91. Secondly, we substitute $k_z=q\pi/L$ (L is the cavity length) into the FEL resonance condition $\omega=(k_w+k_z)\langle v_z\rangle$ to determine the averaged axial velocity $\langle v_z\rangle$ needed for 17.12 GHz. We obtain $\langle v_z\rangle=0.924c$. Thirdly, we determine the axial magnetic field by passing an electron with a zero initial radial coordinate through the wiggler magnetic field and making the electron have an averaged axial velocity of $0.924c$ and we obtain B_0=5000 Gauss. Finally, we run RKFEL to make the output power maximum by modifying the axial magnetic field and we obtain B_0=5100 Gauss. As a consequence, the averaged axial velocity also has been modified to $0.926c$. Because of the transverse gradient effect of the wiggler field, the axial velocities for the electrons far away from the wiggler axis have larger oscillations, as shown in Fig. 2.

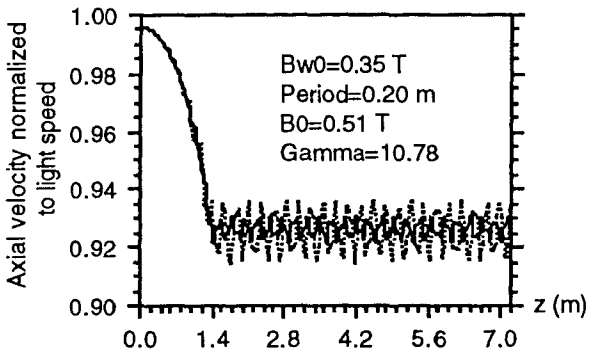

Fig. 2. Axial velocity versus distance. Initial radial coordinates=0 mm (solid) and 4 mm (dashed).

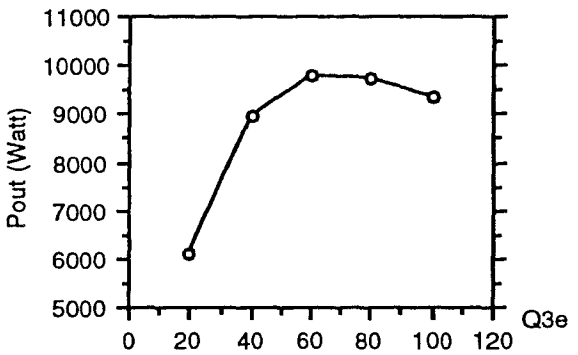

Fig. 3. Dependence of output power on external quality factor for a 2-ns beam pulse.

According to analytical calculation,[9] the wall-dissipated quality factors for the three cavities are all taken as 2×10^5. Taking the effect of beam loading into account, we set the external factors for the first two cavities $Q_{1e}=Q_{2e}=300$. For the third cavity, Q_{3e} is taken as 60. The dependence of the output power on Q_{3e} for a 2-ns beam pulse is shown in Fig. 3.

4. SIMULATION RESULTS

We ran RKFEL for the three-cavity FEL, described in the previous section, with a 4-mm radius electron beam. Figure 4 shows the input beam energy and current. The 50-ns pulse has a 5-ns rise time, 40-ns flat top, and 5-ns fall time. Figure 5 shows the rms-beam radius and the beam envelope radius** as functions of the axial distance z. Both the rms-radius and envelope radius exhibit wiggle motion. Because of the electron wiggle motion, the envelope radius is greatly increased after the beam enters the wiggler region. Figures 6 and 7 show the dependence of the transverse averaged RF current densities $\langle J_x\rangle$ and $\langle J_y\rangle$ on axial distance at t=45 ns, where $\langle J_{x,y}\rangle=\int J_{x,y}dxdy/\pi r_{rms}^2$ with r_{rms} the beam rms-radius. Before the first cavity, there is no transverse RF current. From the first cavity on, the transverse RF current is gradually increased. Figure 8 shows the axial RF current as a function of axial distance at t=45 ns. Because of the longitudinal bunching in the FEL, the longitudinal RF current can reach up to above 800 Amp. However, the longitudinal current can not interact with the RF field. Figure 9 shows the time profile of the output power extracted from the third cavity. It is seen that the output power pulse has a quite long rise time, which shows that a SWFEL is not good as a few-cavity power source (compared to a RK) although it is still interesting in a TBA.

** In the three-dimensional wiggler field, the electron beam is not symmetric about the wiggler axis, and the beam cross-section for different axial distances lies in different position on the plane perpendicular to the axis. Here the envelope radius is defined as the largest radial distance of the electrons in the beam cross-section. For an axisymmetric beam cross-section, the envelope radius is equal to the beam radius under this definition.

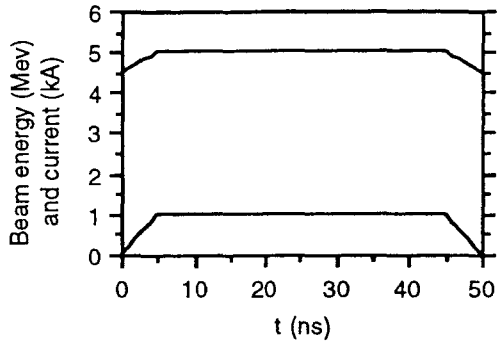

Fig. 4. Beam energy (upper) and current (lower) versus time.

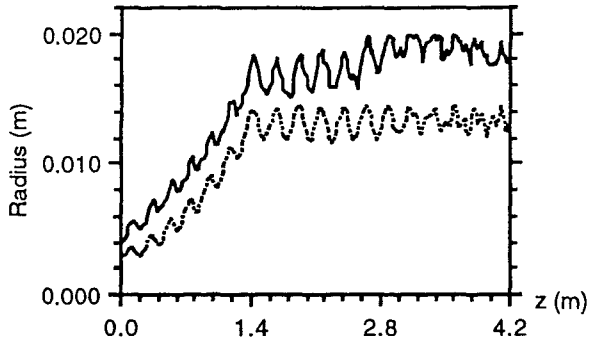

Fig. 5. Envelope radius (solid) and rms-radius (dashed) versus distance.

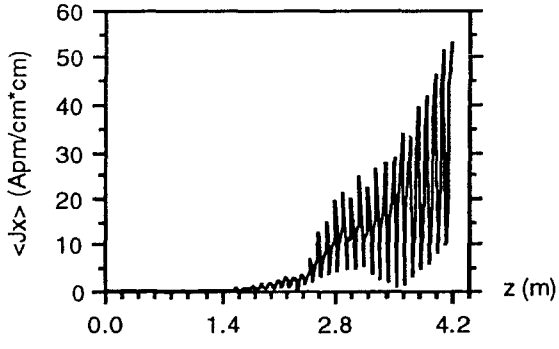

Fig. 6. Averaged transverse RF current density <Jx> versus distance (at t=45 ns).

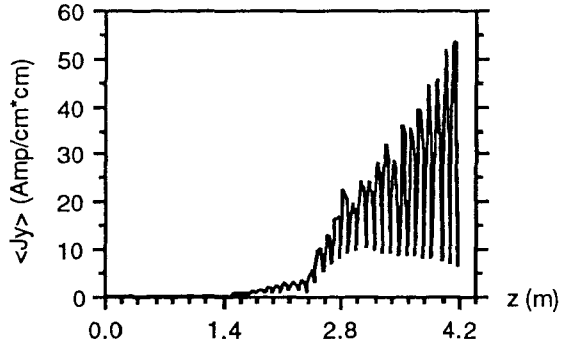

Fig. 7. Averaged transverse RF current density <Jy> versus distance (at t=45 ns).

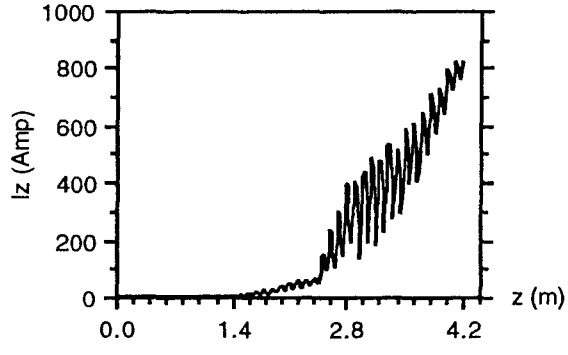

Fig. 8. Axial RF current Iz versus distance (at t=45 ns).

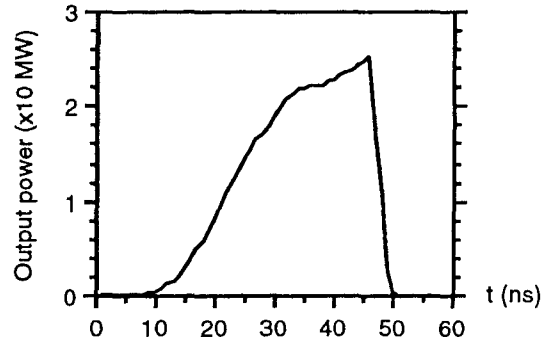

Fig. 9. Output power versus time.

5. BEAM RADIUS EFFECT

To examine the three-dimensional effect of the wiggler field and the RF field on the RF output power, we ran RKFEL with different beam radii. Figure 10 shows the dependence of beam envelope on axial distance for the initial radii 0.5 mm, 2.5 mm, and 4.0 mm. The beam with a smaller intial radius has a smaller envelope radius in the interaction region. The maximum envelope radius r_b at the entrance of the first cavity is 1.4 cm for the 0.5-mm radius beam, 1.6 cm for the 2.5-mm radius beam, and 1.8 cm for the 4.0-mm radius beam. Their values of $k_w r_b$ are, respectively, 0.44, 0.50, and 0.57. Figure 11 shows the output powers as functions of time for the three beams. The smaller the beam radius is, the larger the peak power is. The peak output power of the 0.5-mm radius beam is about three times that of the 4.0-mm radius beam. However, the transit time of the output power pulse of the 0.5-mm radius beam is so long that its ouput power does not have enough

time to reach saturation. From this we can see that the three-dimensional effect is important when $k_w r_b$ larger than 0.5 although the initial beam radius is quite small compared to the wiggler period.

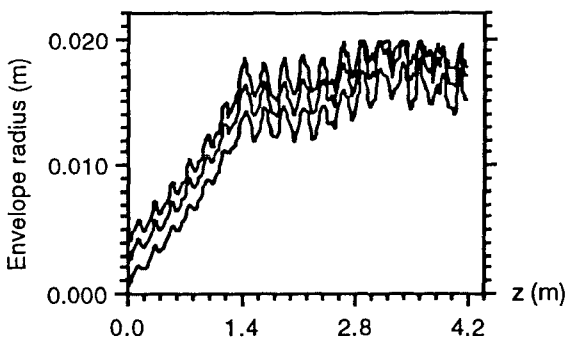

Fig. 10. Beam envelope radius versus distance for beam radii=0.5 mm (lower), =2.5 mm (middle), and =4.0 mm (upper).

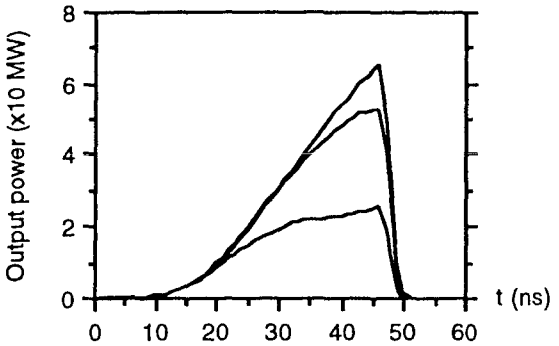

Fig. 11. Output power versus time for beam radii=0.5 mm (upper), 2.5 mm (middle), and 4.0 mm (lower).

6. SUMMARY

The code RKFEL, written based on RKTW2D, has been used to simulate a SWFEL with three cavities and examine three-dimensional effects on the RF output power. It is shown that for an electron beam with big wiggle motion the three-dimensional effect is important although its initial radius is small compared with the wiggler period. In our simulations, we also have seen that the RF output power and the efficiency are quite low, and the transit time of the output power pulse is very long. We believe this is because we only have three cavities in our model. In future work, we plan to study a variety of SWFEL structures and, most particularly, employ many cavities and/or a pre-bunched beam.

7. ACKNOWLEDGMENTS

We would like to thank T. L. Houck at LLNL and R. Govil for their good comments and suggestions, and M. E. Conde for his useful discussions. We also wish to thank G. Fiorentini for her assistance.

8. REFERENCES

1. A. M. Sessler, D. H. Whittum, J. S. Wurtele, W. M. Sharp, and M. A. Makowski, "Standing-wave free-electron laser two-beam accelerator," Nucl. Instr. and Meth. Vol. A306, pp. 592-605, Sept. 1991.

2. G. Rangarajan, A. M. Sessler, and W. M. Sharp, "Discrete cavity model of a standing-wave free-electron laser," Lawrence Berkeley Laboratory Report LBL-31197, Aug. 1991.

3. J. S. Wurtele, D. H. Whittum, and A. M. Sessler, "Impedance-based analysis and study of phase sensitivity in slow-wave two-beam accelerators," Lawrence Berkeley Laboratory Report LBL-31848, June 1992.

4. G. Rangarajan and A. M. Sessler, "Sensitivity studies of a standing-wave free-electron laser," Lawrence Berkeley Laboratory Report LBL-32463, June 1992.

5. S. Krishnagopal, G. Rangarajan, and A. M. Sessler, "The multi-cavity free-electron laser," Lawrence Berkeley Laboratory Report LBL-32220, July 1992.

6. R. D. Ryne and S. Yu, "Relativistic klystron simulations using RKTW2D," Proceedings of the 15th Int'l LINAC Conference, Albuquerque, NM, Sept. 10-14, 1992, pp. 177-179.

7. G. M. Fiorentini, T. L. Houck, and C. Wang, "Design of a reacceleration experiment using the choppertron," to be published in Proceedings of SPIE on Intense Microwave Pulse.

8. R. D. Ryne and S. Yu, RK2D User's Manual (Part I Theory), reprint, Aug. 10, 1988.

9. R. E. Collin, Foundations for Microwave Engineering, p. 327, McGraw-Hill Book Company, NY, 1966.